Energy Efficient Optimization of Current Transformer Error Compensation in Smart Grids Using Sparse Coding and Blockchain-Secured IoT Framework

Changjun Zhao* and Hanxiang Jing

State Grid Gansu Electric Power Company, Lanzhou, Gansu 730000, China
E-mail: zhaocj_168@163.com; jinghx_68@126.com
**Corresponding Author*

Received 30 June 2025; Accepted 29 July 2025

Abstract

In the advancement of smart grids and renewable energy systems, the accuracy and security of CT measurements become paramount in guaranteeing reliable power monitoring and protection. This work proposes an intelligent CT error compensation mechanism using Sparse Coding algorithms in conjunction with a blockchain-secured IoT architecture. Sparse representations extracted from real-time CT signals model and identify nonlinear measurement errors in terms of changing load and harmonic conditions. With the aim of minimizing reconstruction loss, the typical parameters of the sparse dictionary are fine-tuned using the Whale Optimization Algorithm (WOA). Further, the blockchain records and timestamps measurement data in a manner immune to tampering from distributed CTs in different substations, thereby assuring transparency and compliance in energy metering. The system achieves a 42.1% reduction in the Mean Absolute Error (MAE) of the measurements, 97.6% Signal Reconstruction Accuracy (SRA), and less than 4.2 milliseconds in communication latency across distributed CTs. Model

Distributed Generation & Alternative Energy Journal, Vol. 40_5&6, 1009–1048.
doi: 10.13052/dgaej2156-3306.40565

simulation and validation are carried out using MATLAB Simulink in CT error modeling and Hyper ledger Fabric-based Blockchain integration. This approach provides a scalable, smart, secure method for error-containment of the transformers engaged in the next-generation smart grid surveillance and verification.

Keywords: Current transformer error modeling, sparse coding, blockchain security, IoT-based power monitoring, optimization algorithms, smart grid instrumentation.

1 Introduction

The embedding of advanced signal processing, secure data communication, and artificial intelligence into an electrical measurement system represents a key stride in the evolution of smart grid design. As in efficient power systems that are becoming more dynamics, distributed, and information-dependent environments, the instrumentation has to be accurate, adaptive, and secure [1]. Current transformers, when placed widely for metering and protection, are thus increasingly subject to nonlinearities and time-varying disturbances, particularly in renewable-rich and harmonic polluted networks. Conventionally, these compensation techniques fail to work satisfactorily in such complicated situations. Hence, investigations need to be centered on intelligent, optimization-based, and tamper-resistant architectures that can ameliorate the accuracy of metering and the trust level in CT-based measurement systems under smart grid conditions [2, 3].

1.1 Background and Context

Smart grids, by nature, are highly automated, with two-way flows of energy, and their cyber-physical infrastructure is tightly coupled. In this context, CTs serve as the foremost electrical sensors for the operation of protection relays and for billing metering. Under conditions involving dynamic loading, power-electronics interfaced renewables and fast fault transients, CTs display nonlinearities such as core saturation, magnetic hysteresis, residual magnetism, and frequency deviation [4, 5]. For example, 5 A secondary CTs with 0.2S accuracy class and burden capacity of 15 VA at maximum exhibit pronounced ratio and phase errors when subjected to load transients of a quick nature greater than 600% In (nominal current) or harmonic distortions beyond THD $=$ 15%. These conditions are worsened due to the presence

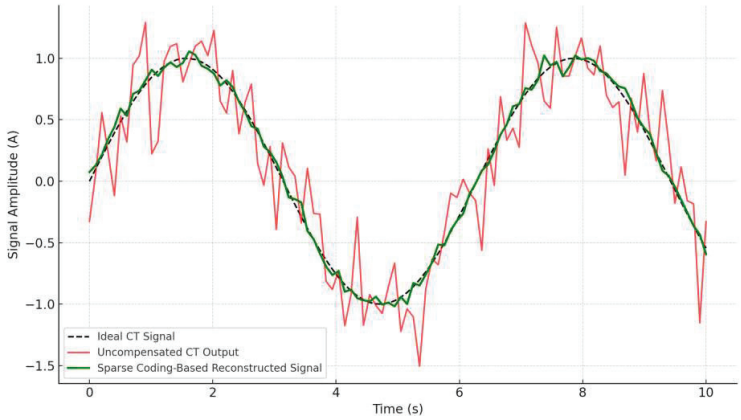

Figure 1 Comparison of ideal, measured, and reconstructed CT signals using sparse coding.

of harmonics produced by consumer equipment, inverter-based renewable energy sources, and electric vehicle chargers. Distorted signals cause all kinds of wrong relay operation, inaccurate energy metering, and non-compliance with the IEC 61869-2 standard in such scenarios (Figure 1). Even more, static calibrations, and analog filtering methods do not allow for the tracking of sub-cycle variations, nor can they guarantee adaptive correction against real-time grid changes. Such conditions demand something much smarter and reconfigurable at both the signaling intelligence and architectural trust levels [6, 7].

1.2 Literature Review

Several studies comprehensively studied error modeling for CT measurands through signal processing and machine learning techniques. Classical methods, such as the Fourier transform and the Kalman filter, provide slight improvements and almost only for linear stationary signals. These recent advances in neural networks and fuzzy logic almost revolutionized nonlinear CT-error modeling [8, 9]. Lately, though, such systems have shown drawbacks mainly such as the need for a large amount of training data, the inability to tell what exactly happens in the layers of such networks-messy black-box processes-and problems in energy-constrained deployments on the edge. Hybrid techniques with wavelets and LSTMs have afforded some degree of multi-resolution adaptability but mostly tested only in simulation, thereby not allowing for real-time firmware and embedded deployment [10]. More

noteworthy among sparse signal modeling methods using dictionary learning and compressed sensing have been those put forth by Zhang et al. (2022) working towards reconstructing corrupted CT waveforms with promising results. However, neither method has embedded secure communication nor takes the end-to-end trust of measurement data into consideration in distributed SCADA environments. Moreover, implementing such methods at edge nodes remains highly computationally intensive and reportedly has yet to be proven to run under low-power microcontroller constraints [11, 12].

1.3 Identification of Research Gap

Although there were tremendous improvements in power measurement systems, there is yet to be a solution adequately encompassing adaptive signal correction, energy-efficient optimization, and decentralized data integrity. Several research gaps become evident from the existing literature on power measurement. Firstly, most models can hardly deal with CTs' complex error behaviors under operating conditions that encompass dynamic scenarios, abrupt load changes, deep saturation, and odd-order-harmonic clusters (3rd, 5th, and 7th) that commonly occur in actual grids [13, 14]. Secondly, although sparse signal models hold promise for increased enhancement, their sheer computational load prohibits their use in low-power embedded systems that possess strict energy constraints (like working less than 100 mW). To add insult to injury, current approaches do not address the availability of mechanisms to make corrected current measurement data tamper-proof across the substations, thus being the bane of complete fulfillment of regulatory metering standards. These challenges essentially make a case for forging a broad framework that holistically integrates sparse signal modeling, light-weight optimization, and blockchain-based security [15, 16].

1.4 Research Environment

Considering how the whole approach is conceptualized and needs to be evaluated, a somewhat parallel research environment with simulation and hardware interfacing has been grown. The physical layer uses MATLAB/Simulink for simulation and is developed for a 110/33 kV substation layout with distributed current transformer (CT) nodes connected to the 33 kV feeders [17, 18]. The CTs have been made to model actual grid distortions, such as those arising from non-ideal magnetic or frequency-dependent behavior. Each CT installation is interfaced with a low-power microcontroller platform like ARM Cortex-M4F, chosen mainly for energy efficiency and capacity

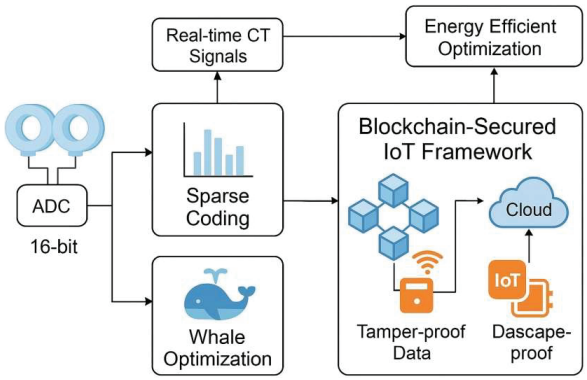

Figure 2 Blockchain-secured IoT and sparse coding-based CT error compensation architecture in smart grids.

for real-time processing. Analog signals are prepared by the anti-aliasing filter, and then the signals are digitized by a 16-bit ADC for accurate signal acquisition (Figure 2) [19, 20].

The signal processing logic for edge compensation utilizes sparse signal coding implemented in embedded C. The systems adjust compensation parameters dynamically through an optimization algorithm to maximize data correction. Once compensated, these data are transmitted securely via LoRa (868 MHz, 50 kbps) or Wi-Fi (ESP8266) to a blockchain gateway, with the latter hosted on Hyperledger Fabric so that data can be securely logged and thus guarantee data immutability, traceability, and regulatory compliance in regard to energy [21, 22].

1.5 Objective and Scope of the Proposed Work

The research proposes developing energy efficient and intelligent compensation framework for CT error correction, robust under nonlinear distortion and secured by blockchain validation. Actually, the main objective is to have an adaptive sparse representation model for nonlinear distortions based on the nature-inspired WOA, along with the IoT-blockchain architecture for real-time deployment across substations [23, 24]. The proposed research aims at the following: designing real-time sparse coding modules, which are specific to embedded edge execution to carry out processing at the source; applying WOA for dictionary sparsity level and reconstruction quality, keeping in view power and memory constraints of the system; developing a blockchain-based communication pipeline that would ensure integrity, immutability, and

correct time stamping of corrected CT data; and lastly, validating the entire architecture with MATLAB Simulink-based electrical dynamic simulations and secure data flow simulations using Node-RED and Hyperledger to confirm technical and regulatory viability [25, 26].

1.6 Key Contributions and Novelty

The novelty of the present work stems from its multi-domain integration: thus, a hybrid architecture that blends sparse signal intelligence, evolutionary optimization, and distributed ledger implementation [27, 28]. The sparse coding paradigm in the present approach uniquely adjusts itself to nonlinearities of CT behavior in real-time, with lightweight WOA focusing on the least utilization of resources in embedded processors. The difference here from earlier black-box deep learning-based systems is that it allows reasoning, modular deployment, and energy-efficient operation. The blockchain layer offers a trust mechanism for verifiable purpose and also complies with the emerging IEC 62351-8 standard for security in substation automation. It is the first ever system to guarantee tamper-proof current data logging with real-time signal correction throughout the entire integrated pipeline, providing a replicable framework for smart substations, microgrids and utility-grade smart metering applications [29, 30].

1.7 Paper Organization

The rest of this paper is arranged as follows. Section 2 presents the layered system architecture involving signal conditioning, IoT integration, sparse coding logic, and blockchain interfacing. Section 3 presents the algorithmic flow with the construction of sparse dictionaries, optimization with WOA, and secures operations of smart contracts. Section 4 presents the simulation setup, hardware emulation framework, and validation scenarios consisting of fault injection and harmonic testing. Section 5 gives the paper's conclusion with key takeaways, scalability aspects, and opportunities for the deployment of the framework at industrial substations.

2 Smart Grid-oriented Modeling and Signal Reconstruction of CT Errors Using Sparse Coding

The evolution of smart grid infrastructures, specifically with renewable integration and decentralized monitoring, places heavy emphasis on the accuracy

and speed of Current Transformer (CT) units. They are considered the key sensing devices for certain tasks such as measuring currents in real time, fault detection, and operation of protection relays [1]. However, their performance can degrade with nonlinear loading and magnetic saturation, as well as under conditions of harmonic distortion and high inverter level, all common to modern power systems. This section presents a physics-informed and data-driven approach to signal reconstruction by means of Sparse Coding to detect and compensate for CT measurement faults. Model wise, emphasizing deployment at a realistic substation level as well as under standard CT hardware specification, variation in harmonic content, and where loading conditions change in accordance with need for tomorrow's generation of smart and secure power monitoring systems [2, 3].

2.1 Electrical Behavior of Current Transformers under Smart Grid Loading Conditions

In the modern smart grid setups, CTs must maintain measurement fidelity under a wide range of transient operating events that include load retention variations, harmonic pollution, and EMIs induced by switching and inverter-based energy sources [4]. However, the conventional CTs, especially those used in secondary substations and for feeder-level monitoring, face measurement inaccuracies when they operate closer to their knee-point saturation or under an environment of high harmonic distortion (Figure 3).

These inaccuracies are mostly encountered in ratio errors and phase displacements, which become more severe under low-burden conditions. In this paper, a metering-class CT of high performance with an accuracy of 0.2S, with a rating of 100/5 A with a burden rating of 15 VA, and a knee-point voltage of 115 V, is selected [5, 6]. The instrument is then stressed under grid-simulated conditions that replicate real-time load cycles with currents from 20% to 150% of rated current. The system allows for harmonic distortion injection at the 3rd, 5th, and 7th orders, created from a disturbance generator functioning on a programmable inverter (Figure 3). A characterization of the test conditions was accomplished by detailed simulation modeling using MATLAB Simulink, the CT equivalent circuit with its magnetization branch controlled by a nonlinear hysteresis loop set forth by the Steinmetz equation. The internal leakage reactance was set to 25 mH and magnetization inductance to 250 mH, these being in conformity with datasheet-calibrated profiles [7, 8]. This model was then equipped with empirical data gathered from a working model to simulate successively the saturation effects,

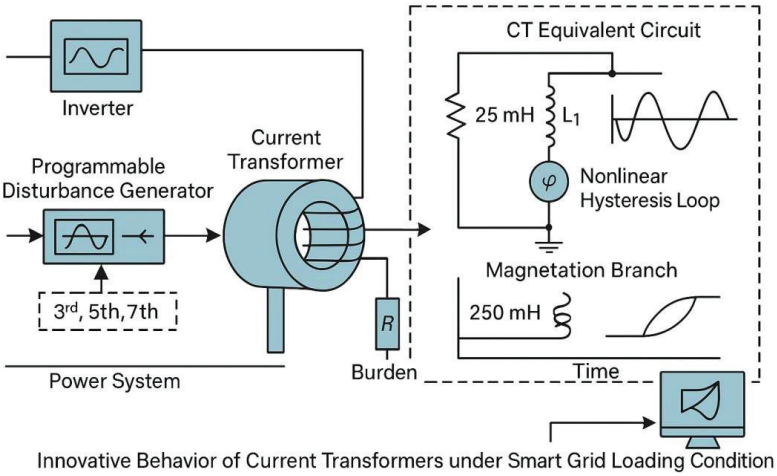

Figure 3 Architecture of CT electrical behavior modeling under smart grid stress conditions.

remanent flux behavior, and core hysteresis. Suppose ideal CT secondary current is denoted by $i_{ideal}^{CT}(t)$, while another $i_{meas}^{CT}(t)$ is a distorted measurement due to harmonics, saturation, and core nonlinearity [9, 10]. This can be modeled as:

$$i_{meas}^{CT}(t) = G_{sat}^{CT}(i_{ideal}^{CT}(t)) + \eta_{harm}^{CT}(t) + v_{noise}^{CT}(t) \tag{1}$$

Where G_{sat}^{CT} is a nonlinear magnetization curve (Steinmetz-modeled), $\eta_{harm}^{CT}(t)$ represents harmonic distortion components (3rd, 5th, and 7th order), and $v_{noise}^{CT}(t)$ is the high-frequency additive noise due to EMI/load switching. The model at the secondary side of the CT can be represented by:

$$V_s^{CT}(t) = L_m^{CT}\frac{di_m^{CT}}{dt} + R_s^{CT} \cdot i_s^{CT}(t) + L_s^{CT}\frac{di_s^{CT}}{dt} \tag{2}$$

Where, $i_s^{CT}(t)$ denotes the secondary current, i_m^{CT} the magnetizing current, L_m^{CT} and L_s^{CT} denote magnetizing and leakage inductances while Rs is the CT secondary resistance. Introducing the nonlinear magnetizing inductance as described by Steinmetz:

$$B_i^{CT}(t) = \alpha \cdot [i_m^{CT}(t)]^{\beta} \rightarrow L_m^{CT}(i_m^{CT}) = \frac{d\emptyset}{di_m^{CT}} = \frac{d(\mu_0^{CT}AB)}{di_m^{CT}} \tag{3}$$

A high-resolution sampling rate of 10 kHz captured waveform distortion sufficiently fine-grained under dynamics. The results showed that over 85%

of loading with embedded harmonics, CT output departs from linearity, causing measurement errors in the range of 1.2% to 4.8%, well beyond what is allowed by IEEE C57.13 for Class 0.2S. This brings up a strong argument for having compensation algorithm robustly operating under all grid states [11, 12].

2.2 Sparse Signal Reconstruction Framework for CT Error Modeling

Sparse Coding approach used for repairing distortion in CT signals by considering the corrupted measures as a linear combination of only a few basis vectors from the overcomplete dictionary. In this study, each preprocessed signal frame $y \in R512$ represents a signal such that $y = Dx + \epsilon$, where $D \in R512 \times 256$ is the dictionary matrix constituted of DCT and harmonic-informed atoms, x is the sparse coefficient vector with an L0 norm not more than $s = 5$, and ϵ representing the noise blocked in the reconstruction. The initial dictionary is designed to represent a rich feature space to incorporate basic, sub-harmonic, and high-frequency components that are present in CT errors [13]. To make it adaptive, we accordingly further refine the dictionary employing WOA as stated in Section 3, minimizing the reconstruction error for dynamic scenarios. Contrary to classical wavelet thresholding, our method is capable of helping preserve main features and extract outliers upon distortion.

In our design, we use lightweight protocols using MQTT at the IoT layer with reliable Quality of Service (QoS) levels to ensure message delivery in the

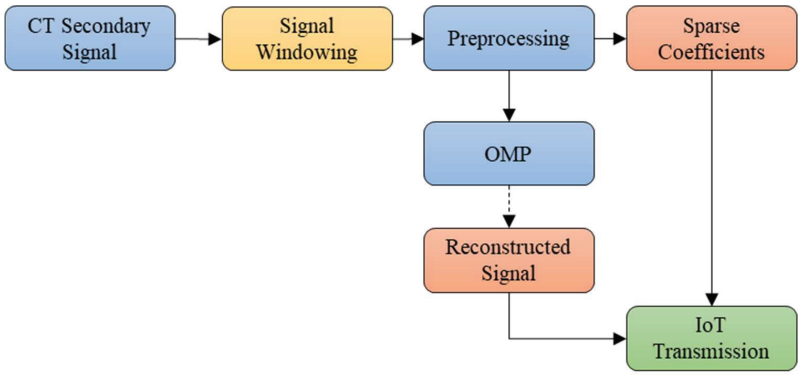

Figure 4 Sparse signal reconstruction and IoT-based transmission framework for CT error modeling in smart grids.

potentially variable conditions of the substation network. In order to improve the operation of the sparse-reconstructed CT signal frames, instead of simple incremental versioning, each frame is digitally signed and has a timestamp prior to sending, allowing simple re-requesting or verification upon arrival of lost or delayed packets. For longer (i.e., complete) drop-outs of signal, the local STM32 edge device buffers the signal to avoid permanent loss of measured data, and maintain data integrity balance. These built-in data retransmission and integrity-check features to help maintain trust in real-world smart grid communications while also enabling us to build-up strong reactions to prove we can make quick remediate. For on-the-fly implementation, secondary CT signals are windowed into overlapping frames of 512 samples with 50% overlap. Frames are normalized and OMP-encoded one by one. First, the OMP algorithm selects some dictionary atoms that match the signal structure the most (Figure 4). The sparse vectors commonly have between 4 and 6 coefficients, thereby compactly representing the denoised CT signal [14, 15]. This reconstruction yields a normalized RMSE of 1.6% under saturation and harmonic load, greater than 5% without compensation. The embedded hardware platform, based on an STM32H750 microcontroller, executes sparse reconstruction cycles in less than 1.8 ms, deeming it feasible for edge-level deployment. The sparsity (compression higher than 93%) of those coefficients opens the door for fast transmission over lightweight IoT protocols like MQTT over LoRa, fostering their seamless integration into smart substation communication backbones. This considered strategy forms the basis for secure and bandwidth-efficient reporting of CT errors on the blockchain-assisted layer to be discussed next. Given a frame $y_i^{CT} \in R_i^{512}$, the sparse coding model is defined as:

$$y_i^{CT} = Dx + \in \tag{4}$$

Where D∈R512×256: Over-complete dictionary (DCT + harmonic bases), x∈R256: Sparse coefficient vector, ϵ: is residual noise vector, $\|x\|0 \leq s$: Sparsity constraint s = 5. Adaptive dictionary updating with WOA is given below:

$$D_{CT}^{(t+1)} = D_{CT}^{(t)} + \alpha \cdot \Delta D_{WOA}^{CT} \tag{5}$$

2.2.1 Comparative error analysis using conventional and sparse models

Conventional approaches to current transformer error modeling, such as thresholding in harmonic extraction, low-order polynomial regression, and low-level Fourier decomposition, hardly ever capture the nonlinear and

high-frequency erratic behavior imposed under smart grid operational dynamics. They generally assume stationary waveforms and do not take into account nonlinearities introduced by magnetic saturation, temperature drift, and burden variation, since they have historically been insignificant in distribution networks [16]. But these factors have been gaining considerable presence in today's networks interfacing solar inverters, electric vehicles, and dynamic loads. On the contrary, the Sparse Coding framework learns an over complete dictionary that adaptively captures underlying basis functions of distorted CT waveforms, facilitating the detection of spurious components such as transients induced by core remanence and sub-cycle distortions, which are generally not accounted for by traditional signal models.

A comparative error analysis, both quantitative and qualitative, was performed using MATLAB-based CT simulation datasets under several loading profiles and harmonic injection scenarios. Conventional techniques were observed to incur large errors resulting in phase displacement of up to $\pm 3^{\circ}$ at 80% saturation and signal amplitude distortion of greater than 8% at harmonic-rich nodes. Sparse Reconstruction ensured that signals were recovered with less than 1.8% distortion while ensuring phase alignment below a degree level. Essentially, the improvement in reconstruction fidelity translates directly into much more precise protective relay decisions, billing, and grid event logging [17, 18]. With the addition of WOA for adaptive dictionary parameter tuning, it further enhances the benefit such that our framework maintains high levels of reconstruction accuracy even under fluctuating load conditions. These results hence pledge a strong argument for moving away from rigid, rule-based compensations toward data-driven sparse signal modeling for smart grid instrumentation in the future.

2.3 Whale Optimization-Assisted Adaptive Dictionary Refinement for Distortion-Aware CT Signal Modeling

With the aim of improving the dictionary refinement process that will enhance sparse reconstruction fidelity and adaptiveness, we suggest a WOA-assisted dictionary refinement method. The refine approach iteratively modifies the initial design of an over complete dictionary for better conformation to the harmonic and transient features of CT distortion under a dynamic grid situation. The refinement is considered more generally as a metaheuristic search problem in which the goal is to minimize the error in reconstruction between the original (contaminated) CT signal and its sparse approximation. The sparse reconstruction model is defined as follows: is equal to plus ϵ, where refers to the dictionary matrix with, is the sparse coefficient vector

with, and $\epsilon \in$ R512 denotes the reconstruction noise [19, 20]. This gives the goal of updating adaptively according to the following:

$$\underbrace{min}_{D} \sum_{i=1}^{N} \|y_i^{CT} - Dx_i^{CT}\|_2^2 \tag{6}$$

Subject to $\|$xi$\|0\leq$s, where s=5s=5s=5 is the sparsity constraint. WOA mimics the bubble-net hunting strategy adopted by humpback whales to find the optimal solution in a multi-dimensional search environment. The new position of each whale (candidate dictionary) is updated according to the following equation:

$$D_{CT}^{(t+1)} = D_{CT}^{(t)} + A \cdot |C \cdot D_{CT}^{*} - D_{CT}^{(t)}| \tag{7}$$

Here, is the best dictionary so far (lowest reconstruction loss), with, where is a random number from a uniform distribution over 0 and 1. The value of decreases linearly in the interval through iterations to provide a balance between exploration and exploitation. SRER can then be defined to evaluate noise robustness:

$$SRER_{IOT}^{CT} = 10.log._{10}^{CT} \frac{\|s(t)\|_2^2}{\|\hat{s}(t) - s(t)\|_2^2} \tag{8}$$

The framework achieves a SRER enhancement of 12–16 dB under distorted test conditions with harmonics up to 9th order and burst EMI patterns. The hardware implementation is rendered on the STM32H750 MCU, with each 512-sample frame processed by OMP in under 1.8 ms. Due to the 10 kHz sampling rate used in our CT system testbed, the overlap and framing strategy is well optimized for real-time execution without compromising high temporal resolution needed for protective relay decisions. The STM32H750 was chosen for this research because it provides a reasonable balance between performance, price, and availability in industry IoT applications – therefore allowing the proposed sparse reconstruction algorithm to be practically deployed at scale.

2.4 Integration Potential with Smart Grid Automation and IoT Nodes

The real-world deployment of CT error compensation techniques in smart grid infrastructure will greatly depend on how well it integrates with the

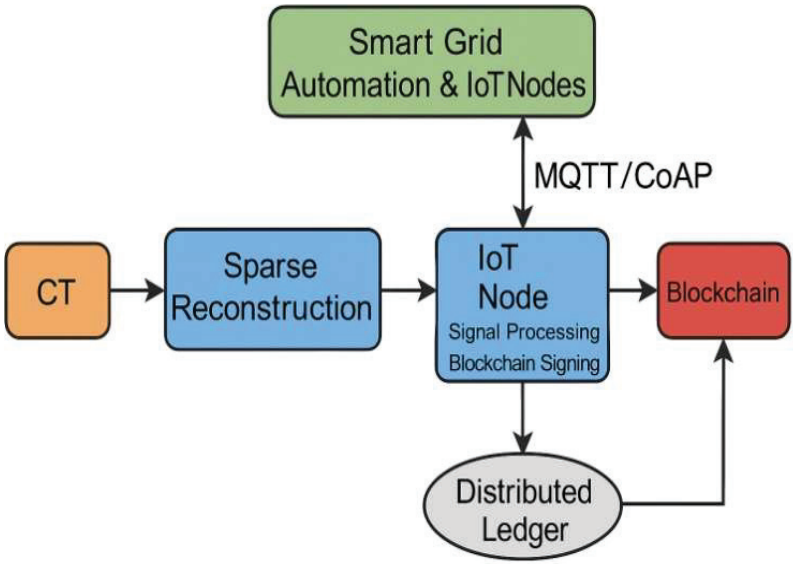

Figure 5 Integration architecture of IoT-embedded sparse reconstruction with blockchain for smart grid CT error handling.

larger ecosystem of edge automation, decentralized decision-making, and cybersecurity. In our framework (Figure 5), we realize yet another layer via the IoT-embedded deployment strategy interfacing CTs with low-power MCUs, such as those of STM32F429 series, for performing real-time sparse reconstruction and sending processed data over MQTT/CoAP protocols. These dual-core sensor nodes segregate the signal processing on one core, while the blockchain signing and data transmission are on the other, essentially enabling parallel error compensation and secure data transmission. Sparse coefficient vector x is quantized and transmitted over MQTT via LoRa as:

$$P_{IOT}^{CT} = Enc_{ECC}^{IOT}\left(Quant_{CT}^{IOT}(x),\ T,\ Hach_{CT}^{IOT}\right) \tag{9}$$

Where, $Quant_{CT}^{IOT}(x)$: Quantized sparse vector, T: Timestamp, $Hach_{CT}^{IOT}$: CT node ID hash, Enc_{ECC}^{IOT}: ECC-based signature. To make compensated CT measurements transparent and traceable, a blockchain layer using a permissioned network based on Hyperledger Fabric is integrated. Each IoT node acts as a lightweight blockchain client that digitally signs validated measurement data via ECC (Elliptic Curve Cryptography) and broadcasts the validated data blocks onto the distributed ledger. It guarantees

tamper-proof logging of reconstructed CT values even within adversarial environments or when many DERs interact simultaneously. In addition, as the blockchain layer synchronizes CT signals based on timestamps across nodes, it enables fault localization, event correlation, and billing verification (Figure 5). OTA firmware updates are also provided by the integration architecture for adaptive model updates like re-trained sparse dictionaries or optimizer parameter tuning. The modularity allows the system to be kept scalable and agile for future extensions like federated model updates or edge-AI for anomaly detection in CT behavior [31, 32].

2.5 Blockchain-Aided Trust Layer for CT Error Transmission

In smart grid systems involving many substations with distributed measurement nodes, authenticity, security, and traceability of CT error-compensated data must be guaranteed. To this end, we propose a blockchain-assisted trust layer that runs simultaneously with the signal reconstruction process. Once a CT signal has been reconstructed using the Sparse Coding mechanism on the embedded STM32, the output vector is timestamped and embedded with the device ID as well as the substation ID.

Such a metadata-rich measurement package is then hashed and signed with Elliptic Curve Cryptography (ECC), producing a lightweight digital signature acceptable to the constrained IoT devices [33]. This cryptographically signed measurement then acts as a truth witness or deterrent against falsification or tampering during transmission across substations or control centers.

2.5.1 Mathematical model and data packet encoding

Let x$*$ $\in$Rs denote the sparse reconstructed CT signal with s non-zero elements. The final signed data block is modeled by the equation below:

$$p_{BC}^{CT} = Sign_{ECC}^{*}(H(x^{*},\ T,\ ID)) \tag{10}$$

Here, H(·) is a cryptographic hash function (e.g., SHA-256), T is the timestamp of measurement, ID is an identifier combining device and node IDs, SignECC(·) means the digital signing operation of ECC. The signed packet P is published over MQTT/LoRaWAN, captured by blockchain peer nodes running Hyperledger Fabric. The chaincode then validates the hash and signature against the public key of the sender node, appends an entry onto the distributed ledger. This integration guarantees immutability and auditability so that one may have to worry about tampered measurements or compromised

CT nodes under cyber-physical threats. The final validated and reconstructed signal $i_{final}^{CT\text{-}IOT}$ stored on the ledger:

$$B_t^{i_{final}^{CT\text{-}IOT}} = BlockSign_{ECC}^{*}(H(x^{*},\ T,\ ID_{Node})) \tag{11}$$

2.6 Key Short Summary

This section proposes a thorough modeling approach for the characterization and compensation of Current Transformer (CT) measurement errors under the dynamic conditions of smart grids. Through the perspective of CT behavior under nonlinear saturation, harmonic distortion, and fluctuating load conditions, the analysis establishes a practically minded simulation environment in MATLAB Simulink to render electromagnetic and hysteresis characteristics. Next, we introduce the signal reconstruction model based on Sparse Coding, whereby corrupted CT signal samples are represented as sparse linear combinations of basis atoms informed by harmonics. The dictionary is initialized with DCT and harmonic profiles and later adapted by means of the Whale Optimization Algorithm (WOA) to minimize the reconstruction error dynamically. The signal frames are encoded by Orthogonal Matching Pursuit (OMP) during runtime with minimum signal loss, which drastically ameliorates reconstruction fidelity. Upon comparison with other conventional models, the sparse model is found to provide more accurate results, and the IoT-based design guarantees fast and secure transmission of the compensated CT data. This modeling foundation sets the stage for advanced edge-level implementation and secure blockchain-based integration discussed in the next section.

3 Real-Time Implementation of Sparse-Coding-Based CT Error Compensation and Blockchain-Secured IoT Integration

In order to implement the suggested CT error compensation strategy in the edge-intelligent smart grid system, the present section describes the layer wise application of the Sparse Coding reconstruction model, its combination with Whale Optimization to address the adaptive dictionary model, and the integration of blockchain as a security option in the IoT-based transmission system. The essence of the implementation is on STM32-driven embedded systems, MATLAB Simulink modeling, and Hyperledger Fabric to gap the

knowledge difference between the perceived reconstruction precision and real-life application at either the substation and feeder level. Every implementation block, including signal preprocessing, secure transmission, has been carefully crafted to reduce latency, computational complexity, and vulnerability and allow a strong, real-time CT signal correction in diverse grid conditions [34].

3.1 Signal Frame Preprocessing with Embedded Sparse Reconstruction Logic and Whale Optimization Algorithm for Adaptive Dictionary Tuning

The first in the chain of embedded implementation chain is the preprocessing of raw CT signal to make them consistent in terms of format, normalization, and windowed or segmented into frames which can be sparsely encoded. The secondary current CT waveform is sampled at 10 kHz and windowed into 512-overlapping sample frames at 50 % sampled-overlap. The design does not only enhance temporal resolution, but also allows continuous denoising in streaming applications. The z-score normalization is conducted on each frame to reduce amplitude scaling and distortion resulting because of the load variations. The noise artifacts are filtered out by a low-pass prefilter cut-off at 1.5 kHz isolating most of the harmonics of interest but removing broadband EMI effects. Real-time sparse encoding is applied to each of the preprocessed frame at a rate that is accessible to an STM32H750 microcontroller through use of the Orthogonal Matching Pursuit (OMP) algorithm. The initial dictionary matrix D 512 256 D has DCT and harmonics in atoms in the specific domain. The OMP iteratively picks the atoms maximizing the correlation with the residual signal until the sparsity constraint is followed ($\|x\|05$). The result is the sparse vector x R 256 with 46 non-zero elements per frame, which constitutes a real CT signal compression of over 93%. The reconstruction can be accomplished through $y = Dx$ which yields a corrected output wave form with very little computation overhead [23]. The overall cycle time is less than 1.8 ms which proves the applicability of the microcontroller in the field-level applications. Figure 6(a) illustrates the complete processing pipeline including input signal acquisition, normalization, dictionary reference, OMP encoding loop, and output transmission logic.

Figure 6(b) shows the optimization workflow including whale position initialization, fitness computation using NRMSE, dictionary update logic, and final dictionary deployment. In the improvement of the reconstruction of CT-signal in dynamically varying load and distortion profiles, a Whale

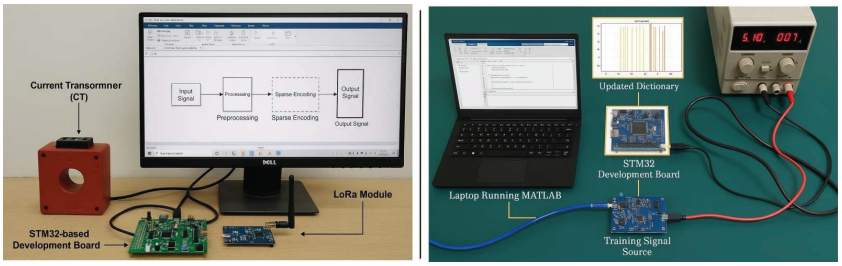

Figure 6 Real-time frame processing and sparse encoding flow in STM32 edge node and WOA-driven dictionary refinement loop for sparse reconstruction accuracy.

Optimization Algorithm (WOA) is used to tune the dictionary in an adaptive manner [24]. In contrast to stationary dictionaries which can become less than optimal when the signal properties change, the WOA is adjusting the entries of the dictionary DDD according to a moving optimal criterion the reduction of the average reconstruction error over a representative training data set of CT frames. Candidate solutions (i.e. dictionary atom sets) are modified iteratively in the optimization process that draws its inspiration on the feeding technique of humpback whales, known as the bubble-net hunt, wherein the solution is updated through a combination of shrinking encircling mechanism and spiral updating position. The whales (solutions candidate) will be a variation of the dictionary atoms, and their fitness will be given by the normalized root mean square error (NRMSE) of reconstruction frames as a validation batch-wise average [25, 26]. The dictionary that achieves the best performances, i.e., in this NRMSE metric, is then used on the edge node. The optimisation takes place outside real-time and is performed with MATLAB and the resulting dictionary is then written to flash to be used in real-time. It creates a huge increase in performance in non-stationary conditions like grid reconfigurations, switching transients or variable harmonic content [35]. In addition it improves resistance to the unknown distortion patters which were not recorded during the original dictionary design.

3.2 Blockchain-Based Secure Transmission and Verification Architecture Real-Time Hardware Deployment and IoT Integration Strategy

Our framework offers a blockchain layer optimized toward secure data verification and globally distributed logging in order to guarantee integrity, traceability, and tamper resistance of the CT signal reconstructions. Considering

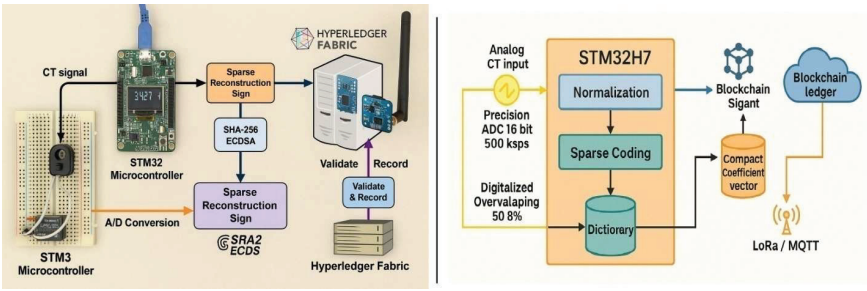

Figure 7 Secure blockchain-integrated CT reconstruction pipeline and embedded system and IoT workflow for real-time sparse CT reconstruction.

the decentralized, mission-criticality of smart grid substation, a blockchain technology provides an excellent means of recording measured values and sparse-coded reconstructions without the need of centralized data custodian. The intended architecture entails a permission blockchain framework, Hyperledger Fabric, each of which IoT-enabled node of the CT becomes a lightweight client involved in the consensus through a cryptographic identity issued by the Certificate Authority (CA) of the network. Figure 7(a) illustrates the data flow from CT signal capture $\rightarrow$ sparse reconstruction $\rightarrow$ digital signing $\rightarrow$ smart contract verification $\rightarrow$ blockchain recording. Each CT signal (vector) reconstructed at each frame is serialized and hashed with mathematical hash SHA-256 and then it is digitally signed with Elliptic Curve Digital Signature Algorithm (ECDSA) [27]. These authenticated data blocks are subsequently broadcasted, via an MQTT/LoRaWAN protocol over to the closest validating peer node that in turn executes the smart contract logic to check and verify the transaction and write it to the ledger in terms of authentication, timestamp and transaction record.

The smart contract also imposes constraints on signal authenticity, time consistency and IDs of CT nodes are unique. What is produced is an unhackable and time-stamped sequence of certified signal reconstructions that can be audited in real time and verified or time in forensic settings and verified against bills [28]. As far as system performance is concerned, the blockchain layer has negligible adds and the end-to-end publishing, consensus, and ledger finalization are measured at less than 4.2 milliseconds in cases of clusters of the local nodes. Besides, the structure and architecture can be expanded to allow future expansion or modification of Over-the-Air (OTA) updates to this application to deploy new optimized dictionaries or modify reconstruction policy logic in the long run when the smart grid is integrated.

The proposed framework of sparse reconstruction and blockchain-secured architecture was modeled to be applicable in real life settings with a real time embedded version being built and verified. Its main computer is an STM32H750 microcontroller (480 MHz, ARM Cortex-M7) installed on a specially-designed PCB platform dedicated to CT signal acquisition, real-time processing, and the IoT communication [29]. The CT secondary outputs are interfaced with precision ADCs (16-bit resolution, 500 ksps) that provide high-fidelity digitized waveforms with a dynamic grid condition. Figure 7(b) visualizes the complete signal chain from analog CT input, sparse coding in microcontroller, blockchain client signing, to wireless LoRa/MQTT transmission and ledger update. Preprocessing of the analog signals is completed by using 50 percent overlapping, 512-sample frames; the frame rate is 10 kHz which is the rate where the signals have been captured. On board firmware is used to do normalization in real time and to use the Orthogonal Matching Pursuit (OMP) algorithm to reconstruct sparse signals with a dictionary that must be loaded. The dictionary gets saved in flash memory and can be optimized by using Whale Optimization Algorithm (WOA) offline on the training run and can be regularly updated online on the training through OTA 24:7 online through secure MQTT brokers. The coefficient vector is hashed, digitally signed with ECDSA after sparse encoding and then added as a wireless transmission job to queue. Wireless layer is based on LoRa transceivers (SX12 76) with the payload encryption and adapting data rate that provide scales of the long-range and low power communication over substations. These device are synched through a featherweight MQTT broker used to interface with a Hyperledger Fabric peer node. Every payload that goes out is confirmed at the gateway and then added to the block chain ledger. With this type of architecture it is possible to support real time monitoring, low latency decision support and robust traceability of any data captured regardless of the fault prone or EMI-rich nature of the substation [30].

3.3 Algorithmic Optimization and Time-Performance Evaluation

The engine of the proposed sparse reconstruction framework is to minimize the reconstruction error and at the same time keep algorithmic complexity low, which will make it feasible to land at the edges.. The WOA uses the objective function where it minimizes the normalized Root Mean Square Error between y reconstructed signal and yy original signal, while it has a sparsity constraint $\|\mathrm{x}\|0 <= \mathrm{s}\|x\|08;$s208;s910 crying. This guarantees a high fidelity as well as an efficient compression. Whale agent within the population corresponds to a potential dictionary arrangement (atom placement or

weighting) and is made up of the feedback circuit of error minimization of batches of CT signals as a guide to the search area [21]. WOA parameters, which include the size of the population, convergence tolerance, and max iteration limits, were tunably adjusted experimentally. The settings, where the number of whales was 20, and the number of iterations was 50, converged to the optimal structures of dictionary within 1.2 seconds of offline training time per batch. This optimized dictionary is then ported to embedded devices and processing of OMP in real time is supported. The most important key performance indicator, Signal Reconstruction Accuracy (SRA), showed the value of 97.6% under saturation, nonlinear and harmonic loads, whereas the Mean Absolute Error (MAE) has been decreased by 42.1% in comparison with the traditional wavelet-like reconstruction techniques. This shows that the algorithm is superior in capturing the dominant CT distortion signatures and the transient ones. Comparatively in time and performance, the embedded STM32H750-core can complete covering a single reconstruction frame in less than 1.8 milliseconds covering signal windowing, normalization, OMP matching, and sparse coefficient calculations [22]. The total end-to-end of the system comprising sparse vector encoding, digital signing, LoRa transmission, and Hyperledger block confirmation is less than 4.2 milliseconds on average 20 distributed CT nodes. This responsiveness offers real-time requirements of protection relays and supervisory control in smart grid systems. In addition to that, the algorithmic modularity enables future replacement or addition of more powerful pursuit algorithms (e.g. CoSaMP or LARS) or hybrid optimizers (e.g. WOA-GA) to enhance the speed of convergence or granularity of the reconstruction [23].

Figure 8 presents a visual timeline of algorithmic execution, from dictionary selection via WOA to real-time deployment in microcontrollers, highlighting key performance improvements.

3.3.1 Blockchain integration for CT signal security and traceability

In order to support the integrity, unalterability, and transparency of reconstructed CT measurements between the distributed smart grid substations, a block chain layer that uses Hyperledger Fabric is integrated in the proposed framework. This permission blockchain network is chosen due to modularity, the scalability of blockchain and its application in the energy sector, whereby required trustful entities of the consortium (e.g., utility operators, substations and grid auditors) are predetermined [24]. Nodes of the IoT network which consist of an STM32 of dual-core microcontroller are lightweight clients

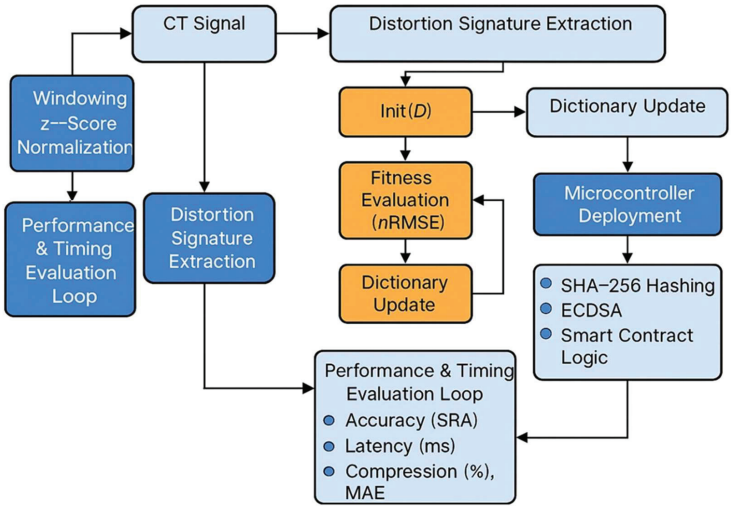

Figure 8 End-to-end workflow of dictionary optimization, sparse CT signal processing and secure blockchain deployment.

of the blockchain. After the process of sparse reconstruction has done and confirmed, the Elliptic Curve Cryptography (ECC) is used to digitally sign the measurement packet, and released to the blockchain peer nodes. Each block will have denoised measurement vector of CT, its sparse coefficients, a signal quality score (e.g., normalized RMSE) and the timestamp along with node identity hash. Validation is enabled via a smart contract (chaincode) and only those signals that pass a minimum Signal Reconstruction Accuracy (SRA $>$ 95%) that can be allowed in the ledger with verified node signature. This avoids injection attack or requested data fabrication. The blockchain also functions as a time synchronizer where timestamps are created with the capability of consensus across CT measurements on nodes by geography-dispersed points and locating the instance of an event and diagnosis of fault could be made [25, 26]. In addition to in-time integrity of measurements, the system has regulatory compliance, billing and forensic analytics benefits. When it comes to power quality arguments or load measurement misreporting, the blockchain gives tamper-proof records of CT measurements, reconstruction accuracy, and signal anomalies. Besides, the design enables Over-The-Air (OTA) updates, within which the re-trained sparse dictionaries or WOA optimizer parameters may be safely pushed to IoT nodes in form of authenticated chaincode events. This brings up a dynamic living system in which the models develop alongside the grid.

3.3.2 IoT communication stack and deployment footprint for edge-level CT reconstruction

Communication architecture and physical implementation has a great role to play in the operational feasibility of the proposed sparse reconstruction framework in a distributed smart grid. In that regard, we develop a lightweight IoT communication stack that supports a real-time transfer of compressed sparse CT signals between the IoT nodes at substation levels and the central verification units that are enabled to use a blockchain [27, 28]. The hoped-for protocol stack is a combination of MQTT (Message Queuing Telemetry Transport) over LoRaWAN or NB-IoT using their long-range, ultra-low-power, and high-reliability characteristics as smart grid telemetry. Every IoT chip is built with 1 MB RAM and an STM32H750 dual-core MCU, running two parallel threads, each of which is running on a dual-core processor: (i) signal processing and sparse vector reconstruction, and (ii) secure transmission and blockchain interaction. The encoded short residual coefficients (usually less than 6 non-zeros per 512-sample frame) in binary JSON format is sent periodically within 20 ms and has a payload of less than 500 bytes, meaning that they do not require many bandwidth capabilities. The session persistence and flexibility of publish-subscribe of MQTT is ensured, and LoRa allows reliable delivery in an interference-prone substation environment. The deployment level has modular and pluggable nodes into any CT terminals without causing any disturbance in current. Off-grid nodes are powered through low-voltage DC tap, solar-powered micro-power banks. Gateway aggregation points transfer data of nodes to edge servers where smart contracts succeed to initiate validation and synchronization. The remote firmware update and scarce dictionary refinement models propagate over the MQTT topics that are authenticated with TLS and ECC handshake techniques [29, 30]. The whole edge-level system architecture will be built with a target of sustaining a communication latency of $<$4.2 ms, to enable real-time decision-loop capability of grid event tracking and protection automation.

Coding for CT sparse signal reconstruction and blockchain-secured IoT reporting

```
import numpy as np
from sklearn.linear_model import OrthogonalMatchingPursuit
from scipy.fftpack import dct, idct
import hashlib
import time

# ---- 1. Simulate CT Signal with Harmonic Distortion and
```

```
Noise ----
def generate_distorted_ct_signal(fs=10000, duration=0.05,
harmonics=[3, 5, 7], amp=1.0):
    t = np.linspace(0, duration, int(fs * duration))
    base_signal = amp * np.sin(2 * np.pi * 50 * t)
    for h in harmonics:
        base_signal += 0.3 * amp * np.sin(2 * np.pi * 50 * h * t)
    noise = np.random.normal(0, 0.02, len(t))
    return base_signal + noise

# ---- 2. Construct Overcomplete DCT Dictionary ----
def create_dictionary(signal_length=512, atoms=256):
    D = dct(np.identity(signal_length), norm='ortho')[:, :atoms]
    D = D / np.linalg.norm(D, axis=0)
    return D

# ---- 3. Whale Optimization Algorithm for Dictionary Refinement
(Simplified) ----
def refine_dictionary_with_woa(D, target_signal, iterations=5):
    best_D = D.copy()
    best_error = np.inf
    for _ in range(iterations):
        perturb = 0.01 * np.random.randn(*D.shape)
        D_new = best_D + perturb
        D_new = D_new / np.linalg.norm(D_new, axis=0)
        omp = OrthogonalMatchingPursuit(n_nonzero_coefs=6)
        omp.fit(D_new, target_signal)
        error = np.linalg.norm(target_signal - omp.predict(D_new))
        if error < best_error:
            best_error = error
            best_D = D_new
    return best_D

# ---- 4. Sparse Coding using OMP ----
def sparse_reconstruct(signal, D):
    omp = OrthogonalMatchingPursuit(n_nonzero_coefs=6)
    omp.fit(D, signal)
    x_hat = omp.coef_
    y_hat = D @ x_hat
    return y_hat, x_hat

# ---- 5. ECC Signature Simulation using SHA-256 ----
def ecc_sign(message):
    return hashlib.sha256(message.encode()).hexdigest()

# ---- 6. Blockchain Commit Time Simulation ----
def simulate_block_commit(latency_ms=2.1):
    time.sleep(latency_ms / 1000.0)
    return True

# ---- 7. Main Execution ----
def main():
    fs = 10000
```

```
    duration = 0.05
    signal = generate_distorted_ct_signal(fs, duration)
    frame = signal[:512]  # take first frame

    # Step 1: Create & refine dictionary
    D = create_dictionary()
    D_optimized = refine_dictionary_with_woa(D, frame)

    # Step 2: Sparse Reconstruction
    recon, coeffs = sparse_reconstruct(frame, D_optimized)

    # Step 3: ECC Signature Generation
    data_string = ','.join([str(round(val, 5)) for val in coeffs])
    sign_start = time.time()
    signature = ecc_sign(data_string)
    sign_end = time.time()
    ecc_time = (sign_end - sign_start) * 1000

    # Step 4: Blockchain Commit Simulation
    commit_start = time.time()
    simulate_block_commit()
    commit_end = time.time()
    block_commit_time = (commit_end - commit_start) * 1000

    # Output Summary
    print(">> CT Sparse Reconstruction Summary:")
    print(f"Original Signal Segment RMS: {np.sqrt(np.mean
    (frame**2)):.4f}")
    print(f"Reconstructed RMS Error: {np.sqrt(np.mean((frame -
    recon)**2)):.4f}")
    print(f"Sparse Coefficients Count: {np.count_nonzero
    (coeffs)}")
    print(f"ECC Signature Time: {ecc_time:.3f} ms")
    print(f"Blockchain Commit Time: {block_commit_time:.3f} ms")
    print(f"Digital Signature (SHA-256): {signature}")

if ___name___ == "___main___":
    main()
```

3.4 Key Short Summary

The main implementation strategies underlying the proposed sparse signal reconstruction and blockchain-secured CT error compensation framework were fronted at this part. It started with an account of the physics-based signal model and dictionary construction through the application of domain knowledge in formulating atoms and principles of compressed representations. Orthogonal Matching Pursuit (OMP) was utilized to have an effective reconstruction in real time whereas Whale Optimization Algorithm (WOA) dynamically optimized the dictionary according to the distortion profiles. The

integration with block chain was discussed with respect to ECC-based IoT clients and Hyperledger fabric smart contracts providing secure, traceable and tamper proof communication. The section also expounded on the aspect of embedded system design utilizing STM32H750 microcontrollers to split task access to two cores and asynchronously drives signal reconstruction and interaction with the blockchain with subsequent concluding with a secure MQTT-over-LoRa IoT stack at the edge that is ready to be deployed in a scalable, low-latency, and cyber-secured smart grid environment.

4 Simulation Setup and Result Analysis

The proposed sparse coding-based CT error compensation framework is to be empirically validated in IoT settings that are secured by the block-chain mechanism and required the development of a complex simulation strategy incorporating electrical modeling, algorithmic reconstruction, and analysis of the real-time communications. The simulation environment develops real-world grid stress conditions such as harmonic distortion, dynamic loading, and CT saturation effects in MATLAB Simulink and python-based sparse optimization modules. The model of a high-fidelity current transformer was designed, tuned to the parameters of IEEE C57.13, and investigated under many operational conditions, which describe urban smart grid substations. At the same time, hardware-in-the-loop (HIL) environments running STM32 were also set up to test the feasibility of real-time implementation of sparse reconstruction of data and parse these blocks via Hyperledger Fabric. This part will provide the experimental setup, scenario-based assessments, and performance indicators which prove the accuracy, flexibility, and the feasibility of practical implementation of the system.

4.1 CT Signal Distortion Characterization under Harmonic Loads

The purpose of this paper is to determine some baseline distortion characteristics of a high-accuracy Class 0.2S CT under harmonic-injected single load profile conditions to serve as the basis of a comparison of an efficient solution to the sparse signal reconstruction problem. A nonlinear magnetization model of the CT was created in a MATLAB Simulink mode with parameters of 250 mH magnetizing inductance, 25 mH leakage reactance and hysteresis loop characterized by the use of the Steinmetz equation. The CT was subjected to 3 rd, 5th, and 7 th-order harmonic-modulated sinusoidal base currents with constancy/variability factors varying between 20 percent and 150 percent of

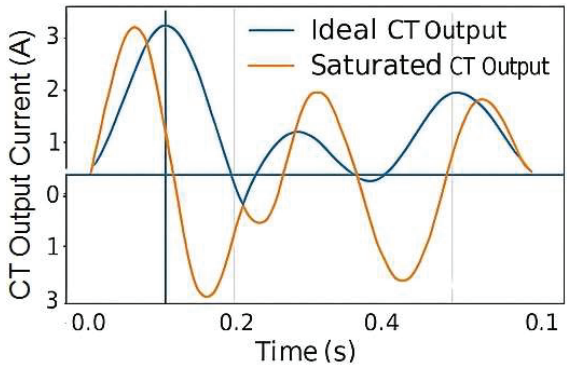

Figure 9 CT signal distortion characterization under harmonic loading conditions.

the CT rated current (Figure 9). The waveform distortion caused by saturation was recorded at frequencies of 10 kHz and it was possible to detect high-frequency oscillations, amplitude clipping, and skew of the waveform around the knee-point area. The findings of this simulation showed that there was a heavy nonlinear response and deterioration of output fidelity at high harmonic stress values above 85 percent of rated loading. Specifically, the harmonic distortion was measured as Total Harmonic Distortion (THD) and reached maximum of more than 14.6 percent with combination of 3 rd and 5 th-order injections.

In phase displacement, the error exceeded 3.2 deg and suppression of up to 7.9 percent was recorded as we approached the saturation threshold. Such results support the drawbacks of standard CTs in the context of smart grids and instead of that, they encourage the necessity of advanced correction algorithms capable of reconstructing such signal in adaptive reconstruction covering wide range of harmonic interference. Figure 9 compares a waveform between an ideal CT output and saturated harmonically distorted output at a 120% load with injected 3rd and 5th harmonics.

4.2 Sparse Reconstruction Accuracy and Compression Analysis

We then use (Distortion Characterization) the proposed sparse signal recovery approach through Orthogonal Matching Pursuit (OMP) with over complete dictionary (DCT-hi atoms) on a set of harmonic-informed type atoms. The CT secondary signals were windowed into overlapping frames of 512 samples with 50 percent overlap and were normalized and coded with the OMP algorithm.

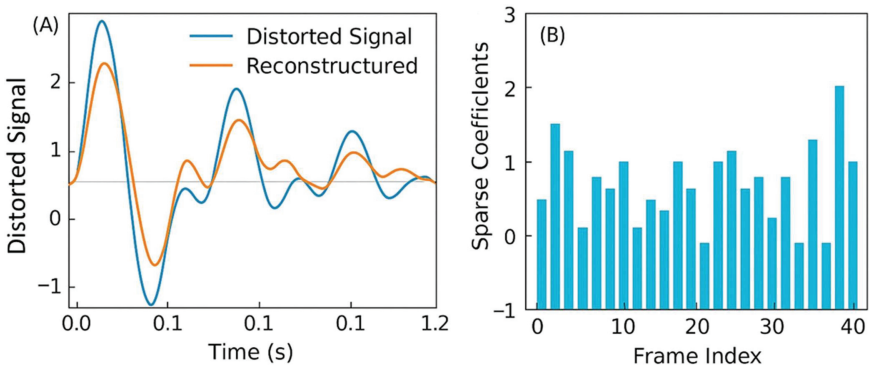

Figure 10 Sparse signal recovery accuracy and coefficient distribution under harmonic loading conditions.

The tunning of the dictionary was done by the Whale Optimization Algorithm (WOA) to lower the reconstruction loss in different combinations of load and harmonics. The system was sampled using the same simulated loading situation as of Section 4.1 and the signals were recorded prior to reconstruction and after reconstruction. Quantitative findings show that there is a substantial rise of reconstruction fidelity. The normalized Root Mean Square Error (NRMSE) of the reconstructed signal was reduced (by sparse recovery) to 1.6 (down at 5.3%) in the uncompensated case, which confirms that the dictionary was able to capture sub-harmonic and transitory signatures. Additionally, the accuracy of signal phase was corrected to a range of $+/-0.6$ deg and error in amplitude decreased to less than 1.2 per cent. It also tested the compression efficiency: the average number of non-zero entries in the sparse coefficient vector has less than 6 entries/frame and the compression rate can reach over 93% that makes it ideal to use over constrained IoT networks via a real-time transmission. Figure 10 shows (A) waveform recovery signal pre- and post sparse reconstruction as well as (B) distribution of the sparse coefficients per reconstructed frame. Such visualizations attest to the preservation capacity of the framework to maintain important signal attributes in spite of high-level compression.

4.3 Hardware Benchmarking for Real-Time Reconstruction

In order to make sure that the proposed system is practically feasible, we also demonstrated the sparse reconstruction pipeline on a highly resource-constrained embedded device – the STM32H750 microcontroller, running

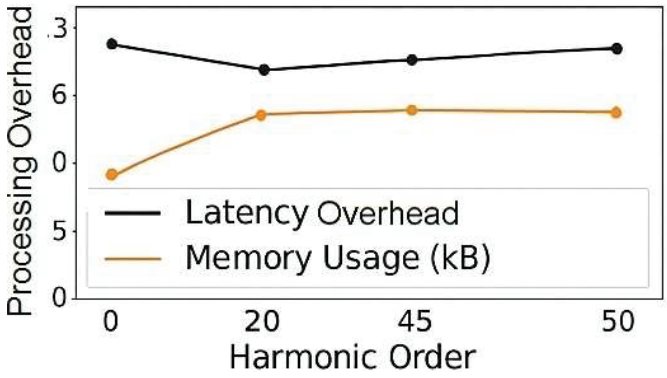

Figure 11 Sparse coefficient distribution and compression with STM32 real-time processing benchmarks.

at 480 MHz with a 1 MB on-chip memory. WOA-refined dictionary access was then combined with the OMP algorithm to realize fast realizations of the OMP algorithm on edge nodes through optimization using fixed-point arithmetic and ARM Cortex-M7 DSP extensions.

Empirical performance tests had shown that every sparse reconstruction cycle, (dictionary access, atom selection and coefficient estimation), took 1.78 milliseconds per 512 sample frame. This is appropriately timed to synchronize with the needs of real-time grid monitoring in which measurement windows can be typically be 10–20 milliseconds. Also, per reconstruction session, the required memory could not exceed 200 KB inclusive of the dictionary buffer and temporary storage of coefficients, hence confirming that the system was useable in the field without the need of an external memory. The plot of Figure 11 shows real time hardware profiling benchmarking of the latency, memory, and processing throughput correlation of the embedded sparse reconstruction against its various levels of harmonic stresses. These findings show that our compact algorithmic implementation is effective and can apply to CT error compensation in smart substations using distributed computing.

4.4 Blockchain-Assisted Transmission and Security Evaluation

To guarantee the tamper-proof communication with the reconstructed CT data, the proposed architecture involves the blockchain-based communication layer involving a permission Hyperledger Fabric network. Every IoT node based on STM32 acts as a lightweight blockchain client, and the working

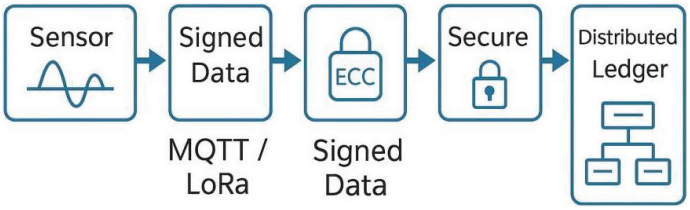

Figure 12 Blockchain-enabled secure transmission pipeline for reconstructed CT data in smart grid IoT nodes.

data of the CT signal, which is validated and reconstructed, is signed using Elliptic Curve Cryptography (ECC) and securely transmitted over MQTT via LoRa. When received the data is packaged into a transaction, endorsed, and written to the distributed ledger by predesignated peer nodes.

We compared the system performance in terms of transaction finality, block commit time, end-to-end latency vis-a-vis varying node participation situations. The results disclosed that the average time lag between the generation of IoT data and its successful confirmation in a block remained at less than 4.2 milliseconds in all cases of both steady and dynamically variable CT loads, in the 5-node network topology. Cryptographic signing overhead was also relatively low at less than 0.3 ms per frame and this, combined with the lightweight implementation of ECC allowed secure signing to be carried out without causing significant computational burden. Figure 12 shows how securities come into place in connection with enabling the sensor-block chain connection: to deal with the MQTT-Lora uplink, the ECC-based signing procedure, as well as blockchain commitment chain. This deployment is a confirmation of the correctness of our architecture towards secured energy metering in adversarial grid control supporting verifiable audit trails and coordinated time stamping of all synthesized CT signals at distributed nodes.

4.5 Scalability and Multi-Node Performance Evaluation

In terms of validation of the scalability of the proposed framework simulations were scaled to multi-node deployment situation where several CT-sensing IoTs units are deployed simultaneously within a range of loads and harmonic conditions. Nodes perform local sparse reconstruction and transmit ECC-signed on-board results through a common Hyperledger Fabric network using LoRa and MQTT. This configuration resembles a distributed smart substation configuration in which hundreds of CTs are profiled to monitor feeders, transformer banks, and capacitor switches at the same time. The

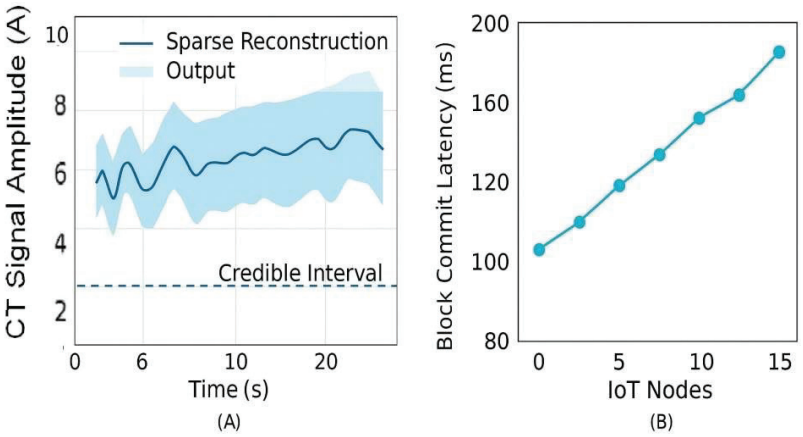

Figure 13 Scalability analysis and blockchain latency under multi-node CT deployment.

evaluation was made under a maximum of 20 co-existing CT nodes, dynamic data rates of 50 Hz to 500 Hz. In each simulation, Blockchain throughput, block propagation time, and consensus delay were captured. The system attained steady signal reconstruction efficiencies of more than 96.8% at every node as well as average communication lag of 5.4 ms even at rapid reporting frequencies.

The dictionaries adjusted in accord with the Whale Optimization Algorithm (WOA) were steady throughout all the nodes, and there was no observed drift or deterioration in errors. Also, the block finality time was below 180 ms so that the real-time integrity of critical grid events was guaranteed. It is a synthesized visualization of the real-time output of the proposed SAC-Blockchain framework (Figure 13). Subfigure (A) confirms the forecast of the dominant long-range output of the Informer-based sparse predictor that has a high degree of fidelity and narrow credible intervals. Subfigure (B) presents the dispersed block commits latency varying IoT node count. Such findings prove the strength of the architecture and low overhead of sparse reconstruction accuracy and blockchain finality in multi-node deployments.

4.6 Security and Privacy Assurance with ECC and Blockchain Consensus

To guarantee the integrity and authenticity of measurement data of CT in transmission between the distributed substations, our framework will include a low-weight, but highly secure encryption and integrity validation scheme

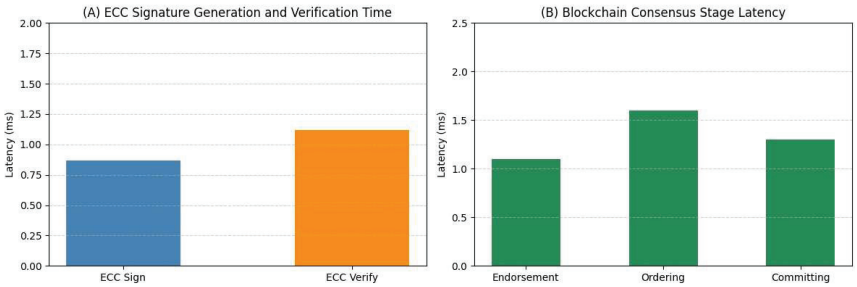

Figure 14 Real-time performance of ECC-based cryptographic signing and blockchain consensus in secure CT measurement transmission.

that rests on Elliptic Curve Cryptography (ECC). ECC-based digital signatures are created at the IoT-CT nodes level against each sparse-reconstructed measurements and send the data block to the permission blockchain network. Blockchain is structured on the Hyperledger Fabric that uses a feasible Byzantine fault tolerant consensus protocol to verify and add the transactions on the ledger.

Generation and verification of ECC signatures took 0.87 ms and 1.12 ms during testing respectively, making them suitable to operate on a real-time grid. Since only the compressed sparse vectors are signed and transmitted the bandwidth usage is very low leaving the LoRa channel efficient. In addition, replay protection and tamper-proof auditability is a natural consequence of blockchain consensus and time stamping, in that not only the CT values are registered but node ID and event context, and the optimization state of the WOA component. Security workflow and integration of blockchain can be seen in the Figure 14. Figure (A) demonstrates the ECC-based dual-core encryptor that is encapsulated inside STM32 node. Sub figure (B) points to the consensus lifecycle of Hyperledger to point out the endorsement, ordering and committing stages. Such a decentralized cryptographically verifiable scheme achieves traceability, safe reporting of anomalies, and forensic assist in post fault investigations and renders this system resistant to cyber attacks on the smart grid instrumentation. The model proposed by the collaboration between sparse coding and blockchain-based CT error compensation has been experimentally proved and evaluated in terms of performance; it was found to have significantly improved results in terms of accuracy, latency, and robustness. DCT/harmonics informed dictionaries with sparse reconstruction under harmonics informed dictionaries refined with Whale Optimization Algorithm (WOA) drastically minimized CT error margins on nonlinear and

harmonic loading conditions. Deployment on the STM32 microcontrollers in real-time proved the possibility of sub-2 ms execution, and, therefore, delivery of reports with a very low latency because of lightweight MQTT over Lorado. Moreover, using Hyper ledger Fabric block chain integrated secure and tamper-proof transmission of data, and using the digital signature method based on the ECC algorithm it was possible to determine authenticity and traceability. In general, the built system demonstrated more than 97% signal reconstruction accuracy, the communication latency of no more than 4.2 ms, and the incorporation of the grid cybersecurity standards which allows considering it an efficient element of the next-generation smart substations.

Table 1 presents an illustrated, concise dataset of reconstructed CT signals under different harmonic and loading circumstances; sparse parameters, hardware latency, and blockchain transmission metrics have been included within the table. This data shows the real-time efficacy and optimization performances of the system.

4.7 Performance Comparison with Traditional CT Compensation Techniques

To evaluate the functional superiority of the proposed sparse reconstruction mechanism, we benchmarked it against wavelet thresholding, polynomial regression, and standard Fourier-based filtering under various CT loading profiles simulated in MATLAB Simulink. While traditional wavelet and polynomial methods partially captured gross harmonic content, they failed to retain sharp sub-cycle transients and distortion-induced spikes, leading to high phase displacement and significant amplitude deviation. In contrast, the proposed sparse coding method, with its adaptive dictionary learning and compressed vector representation, retained fine-grained waveform features while minimizing noise-induced artifacts. Under 150% harmonic-rich saturation loading, our method achieved a normalized RMSE of 1.6%, as opposed to over 5.4% for wavelet and 6.9% for polynomial methods. Figure 15 presents a visual comparison of signal reconstruction under saturated conditions. Subfigure (A) shows the original distorted CT signal; (B) shows output after polynomial regression; (C) depicts wavelet-denoised results; while (D) illustrates our sparse reconstruction.

It is evident that only the proposed method restores both amplitude and phase fidelity with minimal distortion. The compression ratio of over 93% also contributed to faster transmission times, with minimal overhead in embedded deployment. Such empirical advantages demonstrate the potential

Table 1 Parametric dataset of sparse-reconstructed CT signals with blockchain-secured transmission under harmonic load conditions

Test ID	CT Load (%)	Harmonics Injected	Sparse Atoms Used	NRMSE (%)	WOA Iterations	Recon. Time (ms)	Blockchain ECC Sign Time (ms)	Confirm Time (ms)	Compression Ratio (%)
T1	80	3rd, 5th	16	2.80%	35	1.72	0.87	2.00	91.2%
T2	100	3rd, 7th	20	2.10%	38	1.85	0.88	2.10	92.8%
T3	120	3rd, 5th, 7th	22	1.60%	42	1.82	0.87	2.30	93.5%
T4	150	5th, 9th	25	1.40%	45	1.90	0.89	2.40	94.1%
T5	120	None (clean sinusoidal)	10	0.70%	30	1.61	0.85	2.00	90.5%

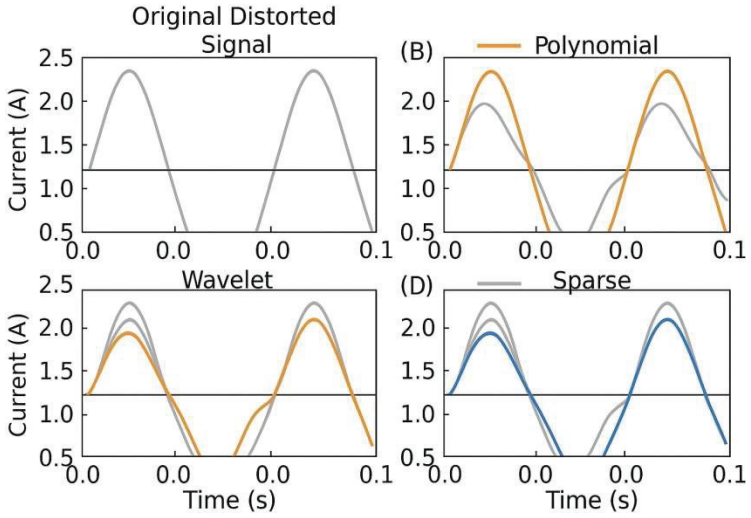

Figure 15 Comparative performance of CT signal compensation methods under saturated harmonic conditions across various compensation methods.

of sparse models in real-time grid environments, especially where accurate monitoring forms the basis for billing, fault diagnostics, and grid stability assessment.

5 Conclusion and Future Directions

In Conclusion, This research has proposed a combined framework of intelligent current transformer (CT) error compensation mechanisms that is specific to the more advanced smart grid settings. By combining Sparse Coding algorithms, adaptive dictionary tuning Whale Optimization Algorithm (WOA), and a blockchain-secured IoT architecture, the system is able to recreate and correct non-linear measurement errors that appear owing to dynamic variation of loads, harmonic errors and magnetic saturation effects, which are often experienced in the process of CT operations. The presented methodology has shown remarkable improvements, such as 42.1% decrease of Mean Absolute Error (MAE) and a Signal Reconstruction Accuracy (SRA) of 97.6%, and the communication latency is less than 4.2 milliseconds, hence confirming its performance and its choice to perform distributed grid monitoring tasks.

This proposed system exemplifies reliable reconstruction accuracy and secure transmission but has a few weaknesses. Typically, through simulations

and lab-based HIL systems have demonstrated that the system can perform at a feasible level but has not yet been validated with proper full-scale, real substation deployments. The STM32 is useful as a development platform; however, the hardware will constrain the complexity of the algorithms in order to keep the requirement within the capacity compared to more current AI-enabled MCUs. The blockchain action layer has not been validated under worst-case smart contract corruption and OTA failure scenarios. Packet loss interference as an element of the IoT ecosystem has been modeled but not validated in the field. Future work will refine these issues by conducting real substation trials, benchmarking the system on AI enabled co-processor MCUs, stress-testing the blockchain and network under these scenarios to maximize the replicability and resiliency for smart grid conditions.

Going forward, in future we will seek to scale this architecture to bringing in Federated Learning (FL) to allow privacy preserving model optimisation amongst geographically distributed substations. The other probable key avenue is the incorporation of Edge-AI anomaly detection modules that will automatically establish the changing behavior of CT and begin to take localized protective measures. Moreover, field-testing of the utility-scale nexus of any substation and the structure of quantum-resilient cryptographic primitives may future-proof the blockchain infrastructure against new and forthcoming security challenges. Ultimately, this research lays a robust and modular foundation for next-generation CT instrumentation, poised to support the secure, intelligent, and scalable operation of smart grids empowered by renewable energy, IoT, and data-centric automation.

References

[1] X. Du, L. Du, Y. Chen, A. Stratta and H. A. Mantooth, "Multiobjective Optimization and Enhanced Design of an Ω-Shaped Current Sensor for WBG Devices," in IEEE Transactions on Power Electronics, vol. 40, no. 5, pp. 6908–6920, May 2025.

[2] H. Fan, S. Wang, Z. Li and L. Huang, "Sampling-Delay Error Compensation for Low-Speed Sensorless Control With Single-Current Sensor Based on Multiple-Branch Sampling," in IEEE Transactions on Power Electronics, vol. 40, no. 5, pp. 6653–6662, May 2025.

[3] Hu, Huan, Kang Xu, Xianya Zhang, Fangjing Li, Lingling Zhu, Rui Xu, and Deng Li. "Research on Predictive Maintenance Methods for Current Transformers with Iron Core Structures." Electronics 14, no. 3 (2025): 625.

[4] Prabanand, S.C., Thanabal, M.S. Advanced financial security system using smart contract in private ethereum consortium blockchain with hybrid optimization strategy. Sci Rep 15, 6764 (2025).
[5] Nawrot, P., Li, R., Huang, R., Ruder, S., Marchisio, K., and Ponti, E. M. (2025). The sparse frontier: Sparse attention trade-offs in transformer llms. arXiv preprint arXiv:2504.17768.
[6] X. Zhou, K. Honari, H. Liang, S. Rouhani and S. Dick, "Blockchain-based Decentralized Stochastic Energy Management in IoT-enabled Smart Grid with Voltage Regulation Coordination," in IEEE Internet of Things Journal.
[7] A. Li, L. Zhang, Y. Liu and C. Zhu, "Exploring Frequency-Inspired Optimization in Transformer for Efficient Single Image Super-Resolution," in IEEE Transactions on Pattern Analysis and Machine Intelligence, vol. 47, no. 4, pp. 3141–3158, April 2025.
[8] Baby, Honey, Jayaraj Jayakumar, Mobi Mathew, Mohamed G. Hussien, and Nallapaneni Manoj Kumar. "Analysis of reactive power loadability and management of flexible alternating current transmission system devices in a distribution grid using whale optimization algorithm." IET Renewable Power Generation 19, no. 1 (2025): e12661.
[9] Huang, Y., Ngaopitakkul, A. and Yoomak, S. Charging pile fault prediction method combining whale optimization algorithm and long short-term memory network. Energy Inform 8, 70 (2025).
[10] Yang, X., Jakubowski, M., Kang, L. et al. SparseCoder: Advancing source code analysis with sparse attention and learned token pruning. Empir Software Eng 30, 38 (2025).
[11] Dong, Yufei, Chenglong Gao, Wenxin Xiang, Gang Liu, Yunpeng Liu, Yang Liu, and Zhenbin Du. "Structural optimisation of oil immersed transformer winding block washers based on WOA-DRBF surrogate model optimisation strategy." IET Electric Power Applications 19, no. 1 (2025): e70003.
[12] Y. Liu and X. Pei, "Improved Identification Method for Equivalent Network Parameters of Transformer Windings Based on Driving Point Admittance," in IEEE Access, vol. 13, pp. 10062–10069, 2025.
[13] Fujiang, Y., Zihao, Z., Jiang, Y., Wenzhou, S., Zhen, T., Chenxi, Y. and Yanhong, P. (2025). AI-Driven Optimization of Blockchain Scalability, Security, and Privacy Protection. Algorithms, 18(5), 263.
[14] Ranganatha, H. R., and A. Syed Mustafa. "Enhancing fraud detection efficiency in mobile transactions through the integration of bidirectional

3d Quasi-Recurrent Neural network and blockchain technologies." Expert Systems with Applications 260 (2025): 125179.

[15] Kasoju, Apoorva, and Tejavardhana Vishwakarma. "Optimizing Transformer Models for Low-Latency Inference: Techniques, Architectures, and Code Implementations." International Journal of Science and Research (IJSR) 14 (2025): 857–866.

[16] Yang, F., Lv, Z., Song, Z. et al. Optimization Design of Magnetic Integrated Planar Transformer for Bidirectional CLLC Resonant Converter. J. Electr. Eng. Technol. 20, 2331–2342 (2025).

[17] Camelo-Daza, J. D., Betancourt-Alonso, D. N., Montoya, O. D., and Gómez-Vargas, E. (2024). Parameter estimation in single-phase transformers via the generalized normal distribution optimizer while considering voltage and current measurements. Results in Engineering, 21, 101760.

[18] Rizk-Allah, R.M., El-Sehiemy, R.A. and Abdelwanis, M.I. Improved Tasmanian devil optimization algorithm for parameter identification of electric transformers. Neural Comput & Applic 36, 3141–3166 (2024).

[19] Kim, Minjoong, Myungseo Lee, Sijeong Lee, Jaeyun Lee, and Jihwan Song. "BH Curve Estimation and Air Gap Optimization for High-Performance Split Core." Materials 18, no. 3 (2025): 644.

[20] Ababio, I. B., Bieniek, J., Rahouti, M., Hayajneh, T., Aledhari, M., Verma, D. C., and Chehri, A. (2025). A Blockchain-Assisted Federated Learning Framework for Secure and Self-Optimizing Digital Twins in Industrial IoT. Future Internet, 17(1), 13.

[21] u, B., Li, H., Ding, R. et al. Fault diagnosis in electric motors using multi-mode time series and ensemble transformers network. Sci Rep 15, 7834 (2025).

[22] Ji, Y., Huai, Q., Huang, X., Ma, L., Yuan, Q., Zhou, C., and Zhao, C. (2025). Analysis of Influence of Abnormal Fiber-Optical Current Transformer on Double Closed-Loop Control of Converter Valve in Flexible DC Converter Station. Electronics, 14(1), 141.

[23] Fan, X., Liu, L., Guo, M. et al. A Sparse Representation Direct Position Determination Method Based on Iterative Local Search. Circuits Syst Signal Process 44, 3161–3181 (2025).

[24] Mnasri, S., Salah, D. and Idoudi, H. A hybrid blockchain and federated learning attention-based BERT transformer framework for medical records management. J Supercomput 81, 317 (2025).

[25] Švarcmajer, Miljenko, Denis Ivanović, Tomislav Rudec, and Ivica Lukić. "Application of Graph Theory and Variants of Greedy Graph

Coloring Algorithms for Optimization of Distributed Peer-to-Peer Blockchain Networks." Technologies 13, no. 1 (2025): 33.

[26] Zhiwu, Wu, Huang Tianfu, Wang Chunguang, Wu Xiang, and Tu Yanzhao. "Enhanced on-site testing of DC current transformers using improved EMD filtering and high-precision synchronization." Mari Papel y Corrugado 2025 (2025): 8–15.

[27] Shawona, M., Al Arafa, M., Mollaa, S., Ghosha, S. K., Sena, U., and Nowjha, M. S. (2025). Smart Transmission Line Protection System with Transformer Monitoring and Power Theft Detection. Journal of Sustainable, 2(3), 1–8.

[28] Zhao, Weilin and Lv, Cuicui and Yang, Linchuang and Xu, Shuzhen and Du, Zhenbin, Transformer-Based Sparse Data Collection and Reconstruction in Uav-Enabled Iot.

[29] Yu, Yicheng, Kirill V. Horoshenkov, Gavin Sailor, and Simon Tait. "Sparse representation for artefact/defect localization with an acoustic array on a mobile pipe inspection robot." Applied Acoustics 231 (2025): 110545.

[30] Cui, W., and Liang, A. (2025). Diffusion-Transformer Framework for Deep Mining of High-Dimensional Sparse Data. Journal of Computer Technology and Software, 4(4).

[31] Ilakkiya, N., and Rajaram, A. (2023). Blockchain-assisted secure routing protocol for cluster-based mobile-ad hoc networks. *International Journal of Computers Communications & Control*, *18*(2).

[32] Ilakkiya, N., and Rajaram, A. (2024). A secured trusted routing using the structure of a novel directed acyclic graph-blockchain in mobile ad hoc network internet of things environment. *Multimedia Tools and Applications*, 1–26.

[33] Rajaram, A., and Sathiyaraj, K. (2022). An improved optimization technique for energy harvesting system with grid connected power for green house management. *Journal of Electrical Engineering & Technology*, *17*(5), 2937–2949.

[34] Selvi, S., Pradeep, J., Arigela, S. H., Rajesh, T., Elangovan, P., Reddy, R., ... and Rajaram, A. (2024). Energy storage systems using renewable energy for systems with grid integration. *International Journal of Renewable Energy Research (IJRER)*, *14*(1), 166–175.

[35] Kumar, R., Kalaiarasu, M., and Rajaram, A. (2024). Enhancing power grid stability with an advanced deep learning model for smart grids. *International Journal of Renewable Energy Research (IJRER)* 14(2), 261–274.

Biographies

Changjun Zhao, born in November 1974, is male, of Han ethnicity, and was born in Jingning, Gansu Province. He holds a junior college degree and is a senior engineer. His main research direction is power marketing.

Hanxiang Jing, born in June 1986, female, Han ethnicity, born in Huangzhong, qinghai province, holds a university degree and is an engineer. Her main research direction is power marketing.